ELSEVIER

Journal of Alloys and Compounds 223 (1995) 22–27

Journal of ALLOYS AND COMPOUNDS

Improved low-temperature dischargeability of C14-type Zr–Cr–Ni Laves phase alloy

Soo-Ryoung Kim [a], Ki-Young Lee [b], Jai-Young Lee [b,*]

[a] *Research Center, Luckey Metals Corp., Mabuk-ri 148-1, Gusung-Myun, Yongin-gun, Kyunggi-do, Korea*

[b] *Department of Materials Science and Engineering, Korea Advanced Institute of Science and Technology, Kusong-dong 373-1, Yusung-gu, Taejon, Korea*

Received 3 June 1994

Abstract

The low-temperature discharge characteristics of C14-type Zr–Cr–Ni Laves phase alloys were investigated. $ZrCr_{1.1}Ni$ alloy shows very good discharge capacity (320 mAh g^{-1}) and cyclic stability (19% of capacity decay after 1000 cycles), but its discharge capacity decreases drastically as the temperature decreases. Considerable improvement in the low-temperature dischargeability was obtained by substituting Mn and V for Cr. This improvement is attributed to the porous Ni-enriched surface and the increased pulverization rate. The low-temperature dischargeability of 1000 cycled $ZrCr_{1.1}Ni$ alloy is much better than that of $Zr(Cr,Mn,V)_{1.1}Ni$ alloy. From surface analysis of the cycled Zr–Cr–Ni alloys it is found that the surface is covered with an Ni-enriched layer formed by the dissolution of Zr and Cr into the KOH electrolyte. The low-temperature dischargeability of the Zr–Cr–Ni alloy can be improved considerably by the Ni-enriched surface layer.

Keywords: Low-temperature dischargeability; Laves phase alloys; Cyclic stability

1. Introduction

In the last decade a number of studies have been carried out to develop metal hydride (MH) electrodes for the Ni–MH battery which has several advantages in comparison with the conventional Ni–Cd battery. The Ni–MH battery contains no toxic materials, has a higher energy density with the same cell voltage, and has no memory effects. The Ni–MH battery is not only a favorable alternative to the Ni–Cd battery for portable appliances, but is also a promising power source for the electric vehicle which requires a higher energy density.

Since the successful improvement of the cyclic stability of $LaNi_5$-based alloy [1,2], AB_5-type alloys have been extensively investigated to improve the overall electrode properties. Recently AB_2-type Laves phase alloys have been of interest because of their higher discharge capacities. The C14-type Zr–Cr–Ni alloy system is promising for AB_2-type electrode materials [3]. These alloys show good discharge capacities and cyclic stability but the discharge capacities decrease drastically at low temperature.

This work concentrated on improvement of the low-temperature dischargeability of Zr–Ci–Ni alloy. At low temperature the discharge reaction depends on the diffusion of hydrogen inside the MH powder and the desorption of hydrogen on the surface.

It is not easy to control the bulk diffusion of hydrogen in MH because hydrogen diffuses through the dislocation pipes which have been generated by the strain on hydriding [4]. By adding alloying elements which increase the pulverization rate, the particle size may be decreased on hydriding owing to the enhanced pulverization rate. It will decrease the diffusion path and increase the surface area. It will be more effective to control the surface reaction by increasing the effective surface area. The metallic Ni layer enriched on the surface is a good catalyst for the hydrogen–hydroxyl reaction as well as a protective layer against KOH electrolyte [5,6]. The Ni-enriched surface layers are known to be formed by dissolution of the other alloying elements [3,6]. In the V–Ti–Zr–Ni alloys [7], the rate capability was improved by adding transition elements and a porous surface was formed after activation owing to dissolution of the transition elements.

The soluble alloying elements were substituted to obtain a porous Ni-enriched surface and shorter diffusion path. Small amounts of Mn and V were sub-

* Corresponding author.

SSDI 0925-8388(94)01499-X

stituted for Cr to improve the low-temperature discharge reactions. The alloying effects as well as the effects of cycling the base alloys on the low-temperature dischargeability are presented with surface analysis (Auger electron spectroscopy (AES) and X-ray photoelectron spectroscopy (XPS)) results of the cycled alloys which showed better dischargeability at low temperature.

2. Experimental details

The $ZrCr_{1+X}Ni$ ($X=0.0, 0.1, 0.2$) and $Zr(Cr,Mn,V)_{1.1}$-Ni alloys were prepared by arc melting in Ar atmosphere and pulverizing to powder (-325 mesh). The structure of the alloy samples was characterized as C14 hexagonal Laves phase by X-ray diffraction. All the alloys were used without any heat treatment.

The pressure–composition isotherms were obtained using a Sievert's type apparatus with 1 g sample in the temperature range 45–60 °C. To prepare an electrode, 0.2 g alloy powder was mixed with 10 wt.% Ni powder (-400 mesh) and 10 wt.% polytetrafluoroethylene binder (-400 mesh), and cold pressed at a pressure of 5 ton cm^{-2}. The electrode was charged and discharged at a constant current of 50 mA g^{-1} in 30 wt.% KOH electrolyte. The cut-off potential of the discharge was -0.75 V with respect to the Hg/HgO reference electrode. The electrode was activated at room temperature after 15 cycles and the discharge capacity was measured in the temperature range from -10 °C to 45 °C and in the current range between 25 mA g^{-1} and 250 mA g^{-1}.

The alloy surface was analyzed by AES and XPS to investigate the influences of the surface conditions on the electrode properties.

3. Results and discussion

3.1. $Zr–Cr_{1+X}Ni$ ($X=0.0–0.2$) alloys

The *P–C–T* curves and the dischargeability results of $ZrCr_{1+X}Ni$ ($X=0.0–0.2$) alloys are shown in Fig. 1(a), (b) and (c). As shown in Fig. 1(a), the desorption curves of the three alloys show no significant differences with respect to the Cr composition, however, the isotherm of the alloy with higher Cr content shows slightly higher pressure at the same ratio [H]/[M]. The calculated discharge capacities of $ZrCr_{1+X}Ni$ alloys are compared with the experimental results in Fig. 1(b). As the Cr content increases, the calculated discharge capacities decrease but the experimental discharge capacities show the maximum value at $X=0.1$.

The discharge capacities of three alloys with respect to the temperature are shown in Fig. 1(c). It is shown that the dischargeability of $ZrCr_{1.1}Ni$ is better than

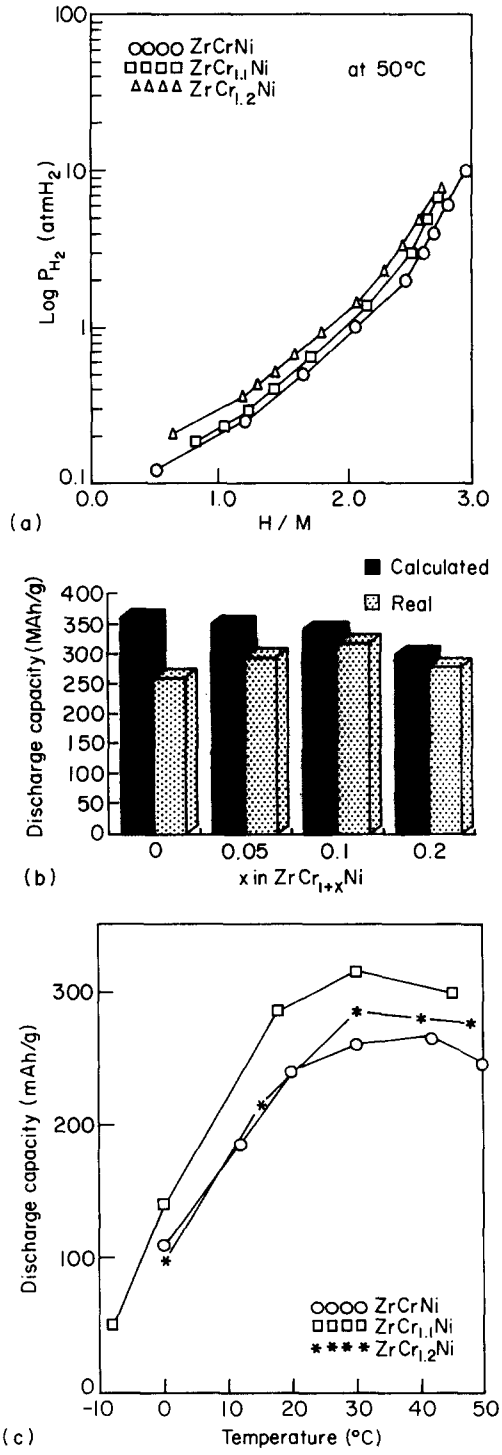

Fig. 1. Thermodynamic and electrode properties of $ZrCr_{1+x}Ni$ alloys: (a) *P–C–T* curves, (b) calculated discharge capacities, (c) dependence of the discharge capacities on temperature.

those of the other alloys in the temperature range between -10 °C and 50 °C. The discharge capacity shows a maximum value at 30 °C. At higher temperature the dischargeability decreases gradually, whilst it drops drastically at lower temperature.

The durability of $ZrCr_{1.1}Ni$ and $ZrCrNiLa_{0.05}$ alloys is shown in Fig. 2. Small amounts of La are added to improve the activation behavior [8]. After 1000 cycles of charging and discharging of the $ZrCr_{1.1}Ni$ electrode the discharge capacity was 81% of the original capacity (320 mAh g^{-1}). For the $ZrCrNiLa_{0.05}$ electrode the discharge capacity after 500 cycles was 89% of the original capacity (300 mAh g^{-1}). Both alloys show almost the same cyclic decay rate. From the results shown in Fig. 1 and Fig. 2, it is found that the durability of the $ZrCr_{1.1}Ni$ alloy is very good but the low temperature discharge capacity is poor.

$ZrCr_{1.1}Ni$ was chosen as a base alloy and small amounts of alloying elements were substituted for Cr, maintaining the C14 Laves phase structure. The low temperature dischargeability is related to the thermodynamic and kinetic characteristics of the alloy. The maximum discharge capacity at a certain temperature is estimated from the hydrogen storage capacity of the *P–C–T* curve in the pressure range between 0.01 atm and 1 atm. This theoretical discharge capacity is restricted by kinetic factors, the diffusion of hydrogen inside the electrode and the desorption of hydrogen on the electrode surface in KOH electrolyte. At low temperature the discharge capacity decreases although the hydrogen storage capacity increases, so the alloy modification is focused on improvement of the kinetic characteristics by modifying surface properties. Cr was substituted by Mn and V to increase the effective surface area of the electrode.

3.2. $Zr(Cr,Mn,V)_{1.1}Ni$ alloys

Cr was substituted by alloying elements such as Mn and V which are soluble in the KOH electrolyte. The *P–C* isotherms of $ZrCr_{1.1-X}Mn_XNi$ ($X=0.3$, 0.5, 0.8) and $Zr(Cr,Mn,V)_{1.1}Ni$ alloys are shown in Fig. 3(a) and (b), respectively. In $ZrCr_{1.1-X}Mn_XNi$ alloys, the hysteresis increases as the Mn content increases. The hydrogen storage capacities of these alloys are smaller than that of $ZrCr_{1.1}Ni$ alloy at 1 atm. The *P–C* isotherm of $Zr(Cr,Mn,V)_{1.1}Ni$ alloy shows very small hysteresis and almost the same hydrogen storage capacity with respect to $ZrCr_{1.1}Ni$ alloys.

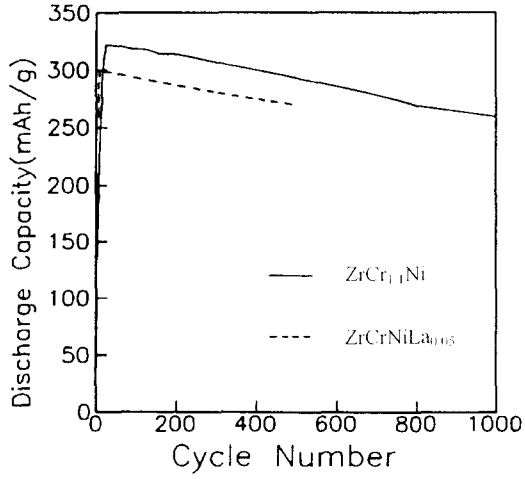

Fig. 2. Cyclic behavior of $ZrCr_{1.1}Ni$ and $ZrCrNiLa_{0.05}$ electrodes.

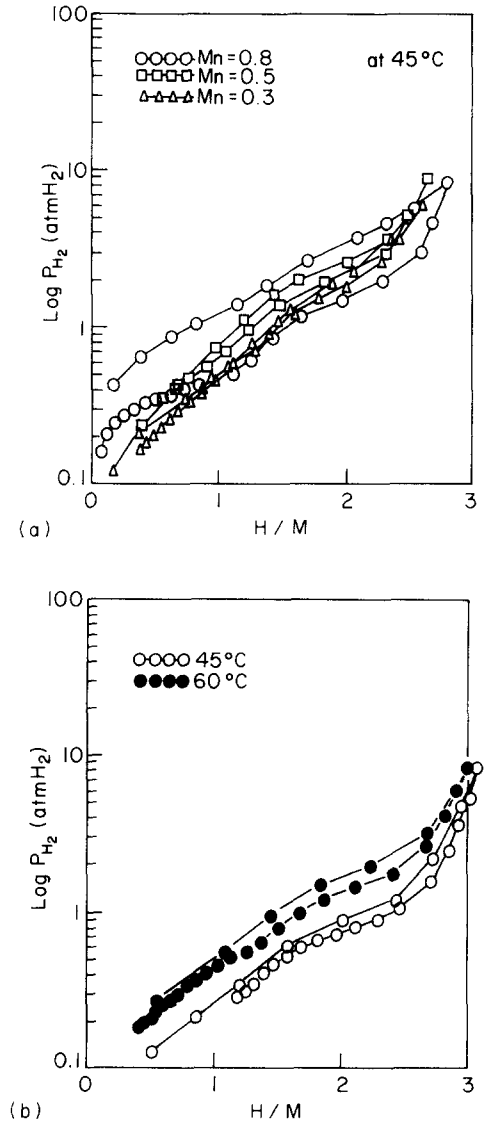

Fig. 3. *P–C–T* curves of (a) $ZrCr_{1.1+X}Mn_XNi$ alloy and (b) $Zr(Cr,Mn,V)_{1.1}Ni$ alloy.

The temperature dependences and the current dependences of the discharge capacity ratio C/C_{MAX} of the four alloys are shown in Fig. 4(a) and (b) respectively. For each alloy, C is the discharge capacity at a certain temperature or current, and C_{MAX} is the maximum discharge capacity. $ZrCr_{0.8}Mn_{0.3}Ni$ and $ZrCr_{0.6}Mn_{0.5}Ni$ alloys show better discharge capacity than $ZrCr_{1.1}Ni$ alloy, and $Zr(Cr,Mn,V)_{1.1}Ni$ alloy shows considerably improved discharge capacity at low temperature. The current dependences of the discharge capacities of the alloys are shown in Fig. 4(b). At higher current, the discharge capacities of the alloys increase in the order

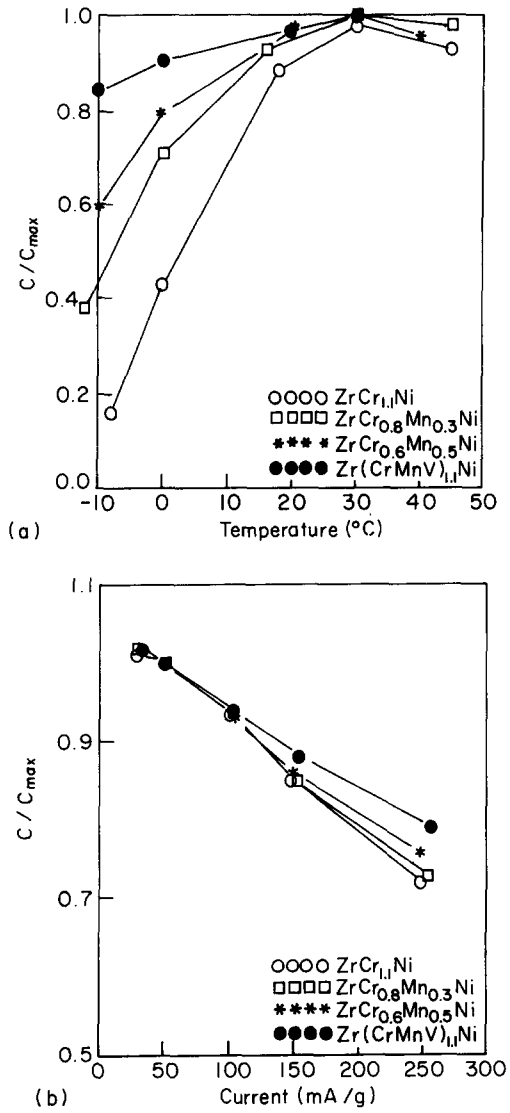

Fig. 4. Discharge characteristics of $ZrCr_{1.1+x}Mn_x$ and $Zr(Cr,Mn,V)_{1.1}$-Ni electrodes: (a) temperature dependence, (b) current dependence.

$ZrCr_{0.8}Mn_{0.3}Ni$, $ZrCr_{0.6}Mn_{0.5}Ni$ and $Zr(Cr,Mn,V)_{1.1}Ni$, but the improvement is not significant.

It is supposed that the improvement in the low-temperature dischargeability is due to the catalytic effects of the Ni-enriched surface as a result of the easy dissolution of Mn and V into the KOH electrolyte, and due partly to the increased surface cracks [3,9] and reduced particle size as a result of Mn which enhances the rate of pulverization of the powder during activation cycles. The enhanced pulverization rate may result in a shorter diffusion path of hydrogen inside the bulk, and the catalytic effects of the Ni-enriched surface will enhance the hydrogen–hydroxyl reaction on the surface.

3.3. Cycled $ZrCr_{1.1}Ni$ alloy

The excellent low-temperature dischargeability of the 1000 cycled $ZrCr_{1.1}Ni$ alloy is shown in Fig. 5 compared

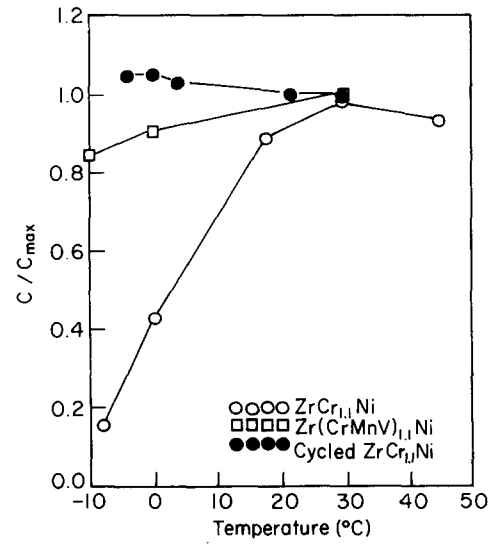

Fig. 5. Temperature dependence of the activated and cycled $ZrCr_{1.1}Ni$ electrodes.

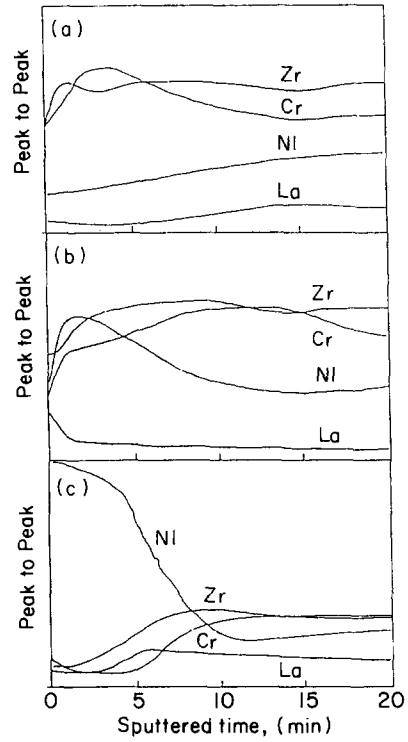

Fig. 6. Depth profile of (a) as-received, (b) activated, (c) 500 cycled $ZrCrNiLa_{0.05}$ electrode.

with the results of activated $ZrCr_{1.1}Ni$ and $Zr(Cr,Mn,V)_{1.1}Ni$ alloys. The discharge capacity at low temperature is almost the same as the value at room temperature.

It is very interesting that the same alloy shows very different results before and after long cycling in KOH electrolyte. As these two samples have the same thermodynamic properties and almost the same pulverization rate owing to the same alloy composition, the only difference is the surface properties.

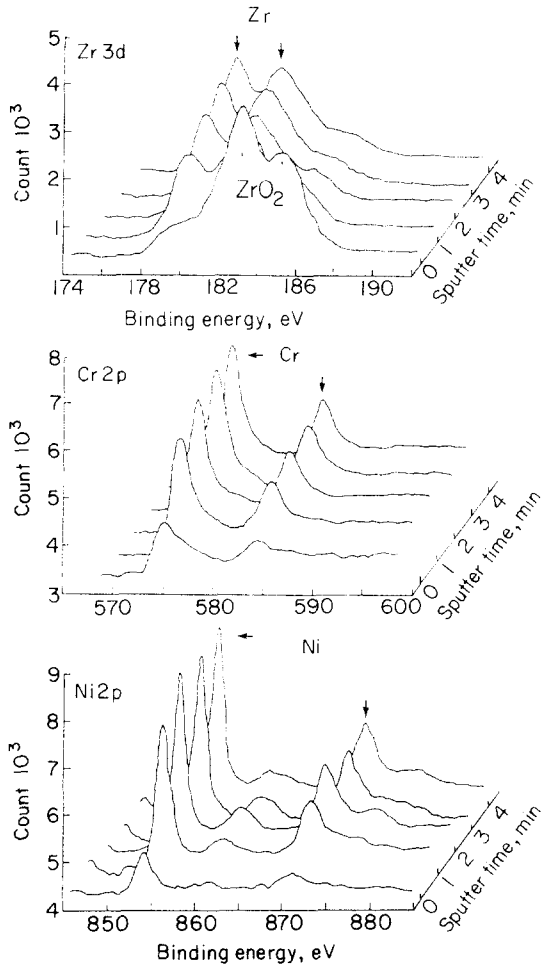

Fig. 7. XPS spectra and depth profiles of as-received $ZrCr_{1.1}Ni$ alloy.

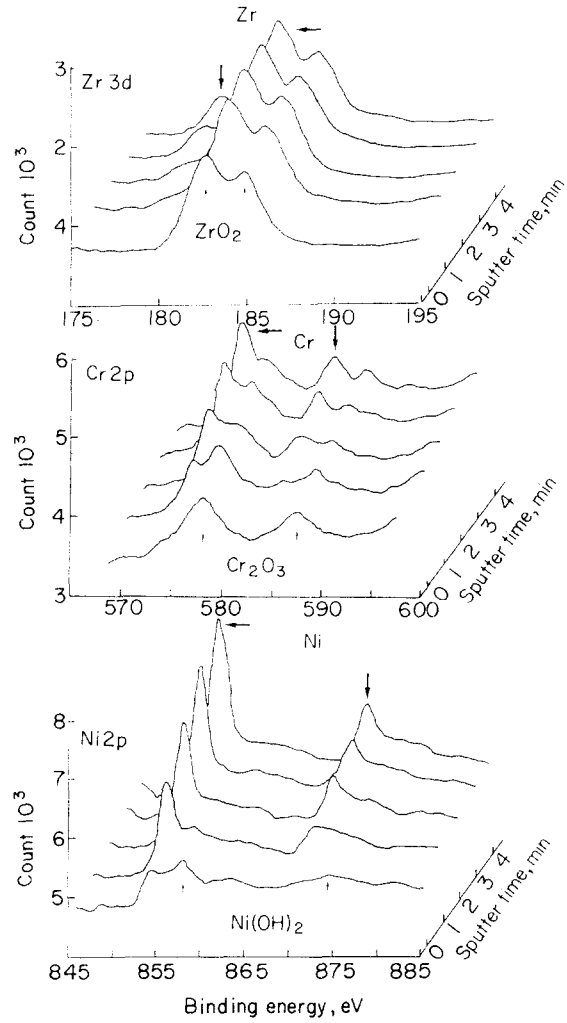

Fig. 8. XPS spectra and depth profiles of 1000 cycled $ZrCr_{1.1}Ni$ alloy.

Surface analysis was performed for the cycled Zr–Cr–Ni alloy with excellent low-temperature discharge capacity.

3.4. Surface analysis (AES and XPS)

The depth profiles of $ZrCrNiLa_{0.05}$ alloy are shown in Fig. 6. The AES analysis was performed for as-received, activated, and 500 cycled samples at a base pressure of 1×10^{-9} Torr with 3 kV and 5 kV Ar^+ ions. For the as-received sample, the surface concentrations of Zr, Cr and Ni are almost the same as the bulk concentration. After activation, the surface concentration of Ni is about twice the bulk concentration, and the surface concentrations of Zr and Cr are smaller than the bulk concentrations. After 500 cycles, the surface concentration of Ni is several times higher than the bulk concentration and the surface concentrations of Zr and Cr are much smaller than the bulk concentration. From the surface analysis, it is found that Zr and Cr have been dissolved into the KOH electrolyte during cycling and the surface concentration of Ni is considerably increased.

XPS surface analyses of as-received and 1000 cycled $ZrCr_{1.1}Ni$ alloys are shown in Figs. 7 and 8 respectively. The samples were sputtered by a 5 kV Ar^+ ion beam with a sputtering rate of 30 Å min^{-1}. Pre-sputtering was performed for 30 s to remove the contaminated surface. About 15 Å of the surface layer was removed during pre-sputtering.

The surface composition of the as-received sample is shown in Fig. 7. No chromium oxide or nickel oxide was observed after pre-sputtering but zirconium oxide (ZrO_2) was observed to a depth of 45 Å. The surface compositions of metallic Zr, Cr and Ni showed a constant value after 2 min sputtering.

In Fig. 8 the surface analysis of a 1000 cycled sample is shown. At a depth of 135 Å, ZrO_2 and Cr_2O_3 were observed. Owing to oxidation the composition of metallic Zr and Cr is lower than that of the as-received sample. $Ni(OH)_2$ was observed on the surface only, and the composition of metallic Ni increased gradually as the sputtering time increased. As there was no reference sample, quantitative analysis was not performed but the metallic Ni layer was observed on the surface after cycling.

From the surface analysis of cycled alloys, it is found that the dissolution of the Zr and Cr resulted in an Ni-enriched surface layer which improved the discharge capacity at low temperature.

4. Conclusion

The cyclic stability of the C14-type $ZrCr_{1.1}Ni$ Laves phase alloys is very good but the discharge capacity at low temperature is not satisfactory. The low-temperature dischargeability of the $ZrCr_{1.1}Ni$ alloy has been improved by substituting soluble alloying elements for Cr or by cycling the electrode for a long time.

The low-temperature dischargeability of $Zr(Cr,V,Mn)_{1.1}Ni$ alloy is improved considerably after activation by substituting V and Mn for Cr. This improvement is attributed to the decreased diffusion path of hydrogen and the increased reactable surface area, which are caused by the reduced particle size due to Mn and the Ni-enriched surface layer due to the easy dissolution of V and Mn respectively.

The low-temperature discharge capacity of 1000 cycled $ZrCr_{1.1}Ni$ alloy was excellent. From surface analysis of the Zr–Cr–Ni alloys, an Ni-enriched layer was found on the surface. It was formed by the dissolution of other alloying elements such as Zr and Cr.

The improvement of the discharge capacity at low temperature is attributed to the increased reactable surface area which can be obtained quickly by substitution of the soluble alloying elements or gradually by cycling the electrode.

References

[1] J.J. Willems, *Philips J. Res., 39* (Suppl. 1) (1984) 1.
[2] J.J. Willems, *Philips Tech. Rev., 43* (1986) 22.
[3] S.R Kim, *PhD Thesis*, Korea Advanced Institute of Science and Technology, 1993.
[4] K.H. Kim, *PhD Thesis*, Korea Advanced Institute of Science and Technology, 1993.
[5] S. Venkatesan, M.A. Fetcenco and S.R. Ovshinsky, *Int. Symp. on Metal–Hydrogen System, Uppsala, June, 1992.*
[6] F. Meli, A. Zuettel and L. Schlapbach, *J. Alloys Comp., 180* (1992) 37.
[7] M. Hirota, A. Wada, R. Nagai, K. Kajita and M.A. Fetcenko, *Electrochemical Society Extended Abstracts, Phoenix, AZ, 13–17 October, 1991,* Electrochemical Society, Pennington, NJ, 1991, p. 172.
[8] S.R. Kim and J.Y. Lee, *J. Alloys Comp., 185* (1992) L1.
[9] S.R. Kim and J.Y. Lee, *J. Alloys Comp.*, to be published.